

Evidence for multiple forms of heritable RNA silencing

Mary S. Chey, Pravrutha Raman, Farida Ettefa, and Antony M. Jose*.

Department of Cell Biology and Molecular Genetics, University of Maryland, College Park, MD 20742.

*Corresponding author: Antony M. Jose

Email: amjose@umd.edu

Author Contributions: MSC, PR, FE, and AMJ designed and performed research. MSC and AMJ wrote the paper with comments from all authors.

Competing Interest Statement: The authors declare no conflict of interest.

Keywords: epigenetics, transgenerational gene silencing, poly-UG RNAs, heredity, gene regulation, operon

Abstract

Heritable gene silencing has been proposed to rely on DNA methylation, histone modifications, and/or non-coding RNAs in different organisms. Here we demonstrate that multiple RNA-mediated mechanisms with distinct and easily detectable molecular signatures can underlie heritable silencing of the same open-reading frame in the nematode *C. elegans*. Using two-gene operons, we reveal three cases of gene-selective silencing that provide support for the transmission of heritable epigenetic changes through different mechanisms of RNA silencing independent of changes in chromatin that would affect all genes of an operon equally. Different heritable epigenetic states of a gene were associated with distinct populations of stabilized mRNA fragments with untemplated poly-UG (pUG) tails, which are known intermediates of RNA silencing. These 'pUG signatures' provide a way to distinguish the multiple mechanisms that can drive heritable RNA silencing of a single gene.

Main Text

Introduction

Epigenetic control systems [1] that regulate the state of an organism evolve along with genome sequence. For a given genome sequence, numerous architectures formed by interacting regulators are compatible with heredity and evolution [2], although fewer may be compatible with particular functions. Nevertheless, detecting and analyzing alternative heritable states of regulatory architectures that can arise for the same genome sequence – i.e., heritable epigenetic changes – remains a challenge.

RNA silencing in the nematode *C. elegans* by double-stranded RNA (dsRNA) or by germline small RNAs called piRNAs can last for many generations without changes in genome sequence (reviewed in [3]). However, the susceptibility to this type of heritable epigenetic change and its transgenerational stability can vary dramatically depending on the target gene [4]. The maintenance of silencing for many generations is thought to require a positive feedback loop that includes the Argonaute protein HRDE-1 [5], which binds antisense small RNAs generated using RNA-dependent RNA polymerases (RdRPs) [6] and mRNA fragments stabilized through the addition of multiple UG dinucleotides (poly-UG or pUG RNAs) [7]. Since HRDE-1 can target nascent transcripts and recruit enzymes that can modify histones [5], a role for chromatin has also been proposed. Indeed, in many organisms, histone modification or DNA methylation is more widely studied in association with heritable epigenetic changes [8]. Here, we show that heritable epigenetic changes can persist even at single genes of operons independent of operon-level chromatin changes and that a diversity of mechanisms characterized by different molecular markers can underlie this heritable RNA silencing in *C. elegans*.

Results and Discussion

Stable RNA silencing that is maintained for hundreds of generations can be induced by mating wild-type hermaphrodites without *mCherry* sequences to males with *mCherry* sequences expressed in the germline either as part of a transgene [4] or fused to the endogenous gene *sad-1* [9]. However, the same *mCherry* sequence fused to the endogenous gene *mex-5* (*mCherry::mex-5* in Fig. 1A) remains expressed and is not susceptible to such mating-induced silencing [4]. To explore the mechanism(s) that promote transgenerational gene silencing, we used Mos1-mediated single-copy insertion (MosSCI) [10] to recreate a transgene that is susceptible to mating-induced silencing. This transgene *T* [4] encodes *mCherry::h2b* and *gfp::h2b* as two genes of an operon (Fig. 1B). Unlike the previously analyzed expressed version of *T* (one of 29% of such expressed isolates [4]), this newly inserted transgene did not show expression of either the *mCherry::H2B* or *GFP::H2B* upon insertion (designated *iTnew* in Fig. 1B; *i* = 'inactive'). As expected [4], loss of the Argonaute protein HRDE-1 resulted in the re-expression of both proteins (Fig. 1B). Although similar insertion of another operon that has the location of *mCherry* swapped with that of *gfp* also failed to show any expression (designated *iTswap* in Fig. 1C), loss of HRDE-1 resulted in the recovery of *mCherry::H2B* fluorescence but not of *GFP::H2B* (designated as *giTswap* in Fig. 1C; *gi* = '*gfp*

inactive). Additional loss of proteins reported as required for heritable RNA silencing (the nucleotidyltransferase RDE-3/MUT-2, the Z-granule helicase ZNFX-1, or the P-granule associated protein DEPS-1) also did not result in re-expression of GFP::H2B. These observations reveal that while *Tnew* is silenced only by an HRDE-1-dependent mechanism (Fig. 1D, *left*), the two genes of *Tswap* are silenced by different mechanisms – one that is HRDE-1-dependent and another that is not (Fig. 1D, *right*). Although the underlying mechanism for this gene-selective silencing is unclear, chromatin-mediated mechanisms or pre-mRNA silencing that impact both genes equally can be excluded.

Similar gene-selective silencing was observed in two other cases: (1) upon ingestion of double-stranded RNA (dsRNA) and (2) upon exposure to expression of a homologous gene.

Silencing by dsRNA has revealed a mechanism for multigenerational gene silencing where the initial production of antisense small RNAs by RdRPs leads to histone modifications by methyltransferases ([11, 12] and reviewed in [3]). Consistently, when exposed to *mCherry*-dsRNA, animals with *T* showed selective silencing of *mCherry* in the exposed parents but silencing of both *gfp* and *mCherry* in descendants (Fig. 1E). These observations support the initial silencing of mRNA in the animals exposed to dsRNA followed by silencing of pre-mRNA and/or modification of chromatin in descendants ('transgenerational epigenetic inheritance (TEI)' in Fig. 1E). In contrast, exposure to *gfp*-dsRNA resulted in selective silencing of *gfp* in the exposed parents and in two additional generations before either recovery or silencing of both genes ('epigenetic recovery' or TEI in Fig. 1F). This selective silencing of *gfp* for three generations reveals an unstable form of heritable RNA silencing that is reminiscent of the 3-4 generations of silencing observed when the endogenous gene *oma-1* is targeted by injected *oma-1*-dsRNA [13].

The stable silencing of *T* initiated by mating is associated with the continuous production of antisense small RNAs that can silence genes of complementary sequence [4] – a phenomenon called *trans* silencing, which has also been observed using other transgenes (e.g., [14]). As expected, when *iT* is introduced into animals with *mCherry::mex-5*, the fluorescence from *mCherry::MEX-5* is not detectable (Fig. 1G, F1 animals). However, in descendants with both *T* and *mCherry::mex-5*, fluorescence from *mCherry::H2B*, but not *GFP::H2B*, recovers (Fig. 1G, F5 animals). This selective re-activation of the *mCherry::h2b* gene in *T* also reveals a mechanism for silencing *gfp::h2b* mRNA without the joint loss of both genes as would be expected for silencing at the level of pre-mRNA or chromatin.

Heritable RNA silencing is associated with the production of pUG RNAs, which are mRNA fragments stabilized by the addition of multiple UG dinucleotides [7]. We used an RT-PCR-based assay [7] where a gene-specific 5' primer and pUG-specific 3' primer are used to amplify cDNA matching the population of pUG RNA sequences made by cleaving mRNA downstream of the start codon (Fig. 2A). Strikingly, we found different populations of sequences were amplified using primers for the *mCherry* gene from each strain (Fig. 2B, *left*). Similarly strain-specific patterns were obtained using primers for *gfp* (Fig. 2B, *middle*), although the patterns were distinct from those observed for *mCherry*. These patterns of pUG RNAs were characteristic of each strain and were largely reproducible when the total RNAs used were prepared from two different populations (Fig. 2C). The presence of detectable pUG RNAs in total RNA from animals that show expression within the germline (*gfp* and *mCherry* from *T* and *mCherry* from *giTswap; hrde-1(-)* in Fig. 2B and 2C) suggests that either pUG RNAs are made within the germline but are insufficient for silencing or that these pUG RNAs are made in a somatic tissue where the *gfp* and *mCherry* sequences are silenced. Therefore, these distinct pUG signatures are molecular indicators of different states of stable expression or silencing for the same open-reading frame. Given the recent discovery that the cleavage of mRNA for pUG RNA production during RNAi of a somatic target gene is restricted to regions that match the dsRNA sequence called pUG zones [15], the different pUG signatures observed could be the result of distinct pUG zones created by different primary triggers of pUG RNA production. However, the underlying regulatory architectures that cause the observed molecular differences are currently unknown.

Since each regulatory architecture can be driven by different epigenetic changes into many alternative states [2], their unambiguous analysis requires keeping track of both genetic and epigenetic states. For example, since the genotypes of *T*, *iT*, and *iTnew* are all the same, they can

be designated similarly using established nomenclature [16] (say, *labSi#* where 'Si' denotes MosSCI insertion). In contrast, their different epigenetic states need different designations (i.e., $\{Epi\text{-}labSi\#(e\text{-}lab1)\}$, $\{Epi\text{-}labSi\#(e\text{-}lab2)\}$, and $\{Epi\text{-}labSi\#(e\text{-}lab3)\}$, respectively; see Strains in Supporting Information for examples and [17] for a discussion). Analyzing the diversity of heritable epigenetic changes that can arise at single genes could reveal the logic of heritable epigenetic effects and enable the design of regulatory circuits with predictable heredity.

Materials and Methods

DNA insertions were generated using MosSCI or Cas9-mediated genome editing. Mutations in known regulators of heritable RNA silencing were introduced through Cas9-mediated genome editing or genetic crosses. Bacteria expressing *gfp*-dsRNA or *mCherry*-dsRNA were used to examine transgenerational dynamics in response to feeding RNAi. Fluorescence from mCherry or GFP fusion proteins in various strains was captured using a Nikon AZ100 microscope and images were identically adjusted using FIJI (NIH). Patterns of pUG RNAs present in total RNA were measured using reverse transcription followed by nested PCR and separating the populations of amplified DNA on a 1% agarose gel. See Supporting Information for detailed materials and methods.

Acknowledgements. We thank Rui Yin for making the plasmid with *Tswap* DNA; Tom Kocher, Bill Snell, and members of the Jose Lab for comments on the manuscript; and the *Caenorhabditis elegans* Genetic Stock Center for some worm strains. This work was supported in part by National Institutes of Health Grants R01GM111457 and R01GM124356, and National Science Foundation Grant 2120895 to A.M.J.

Figures

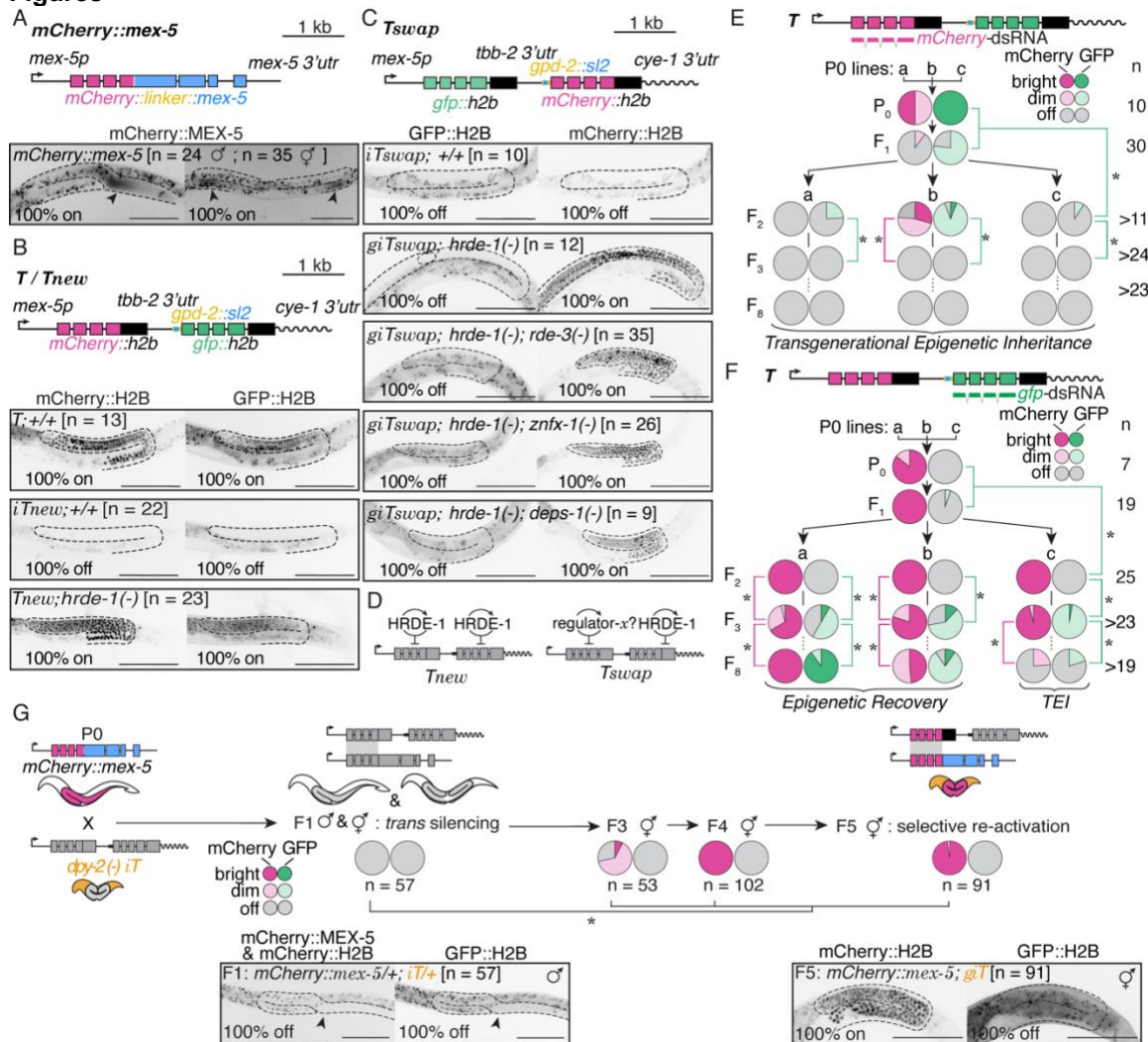


Fig. 1. Gene-selective regulation of an operon can persist for multiple generations. (A-C) Expression from single-copy insertions of *mCherry* and/or *gfp* generated as a fusion with an endogenous gene (*mCherry::mex-5*) or as part of transgenes (*T*, *T_{new}*, and *T_{swap}*). *Top*, Schematics. *Bottom*, Fluorescence (black) of mCherry and/or GFP fusion proteins within the germline (outlined) observed upon insertion of genes, if any, or recovered in various mutant backgrounds (premature stop codons in *hrde-1*, *rde-3/mut-2*, *znfx-1*, and/or *deps-1*). Scale bar = 100 μ m, n indicates number of animals, arrowhead indicates site of *mCherry::MEX-5* accumulation, and intestinal auto fluorescence can be seen as irregular back specks. (D) Summary of observations illustrating *hrde-1*-independent silencing of *gfp* but not *mCherry* in animals with *T_{swap}* versus the *hrde-1*-dependent silencing of both *gfp* and *mCherry* in animals with *T*. (E and F) Transgenerational dynamics of silencing in response to ingested dsRNA matching *mCherry* (E) or *gfp* (F). Fractions of animals showing silencing of each gene in each generation are indicated as pie charts. Lineages can show recovery of expression (epigenetic recovery) or long-term silencing (transgenerational epigenetic inheritance, TEI). Asterisks indicate $P < 0.05$ using the χ^2 test when more than two categories are present or Wilson's estimates for single proportions. (G) The expression of *mCherry::h2b* from *iT* generated by mating-induced silencing is selectively re-activated by *mCherry::mex-5* without re-activation of *gfp::h2b* despite initial *trans* silencing of *mCherry::mex-5*. Scale bars, arrowhead, n, and intestinal autofluorescence are as in (A); asterisks

are as in (E and F). The DNA of *iT* was followed through crosses using a linked *dpy-2(-)* mutation (orange).

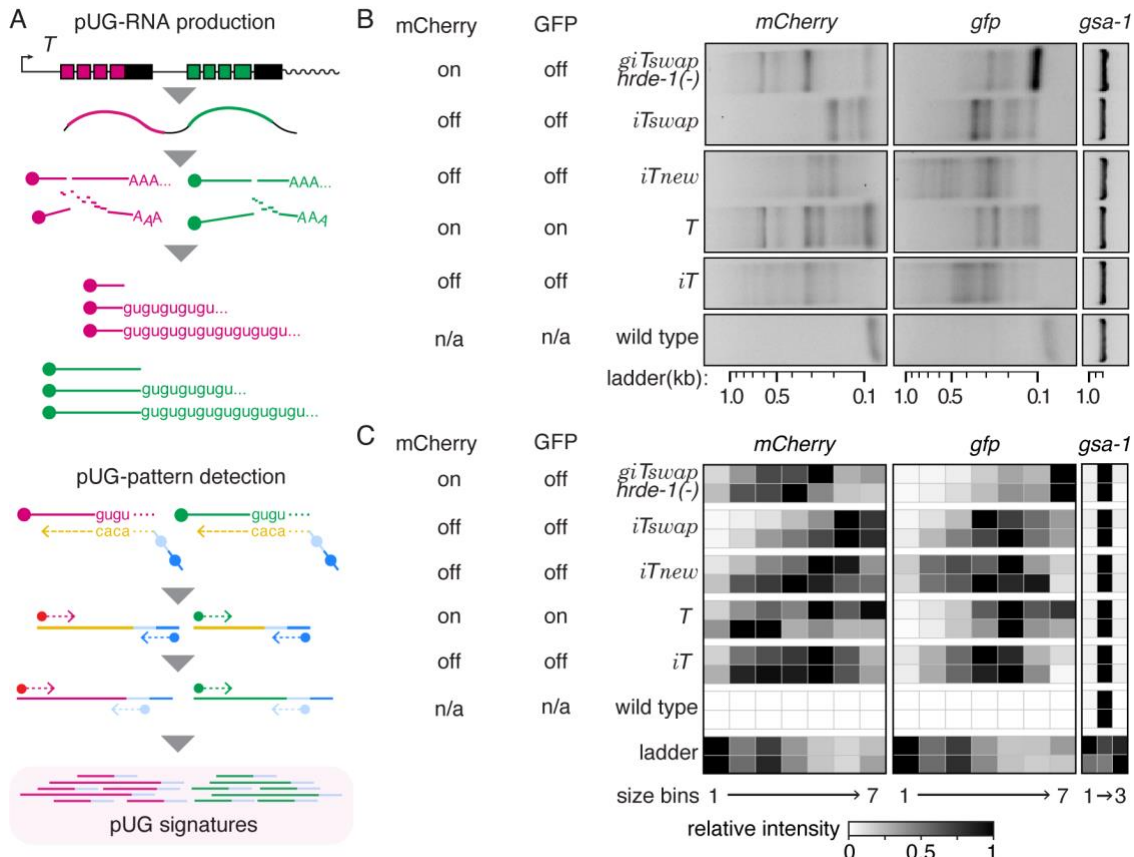


Fig. 2. Heritable RNA silencing of the same open-reading frame can generate distinct populations of pUG RNA. (A) Schematic of pUG RNA production from *T* (top) and the detection of pUG signatures using RT followed by nested PCR (bottom). (B) Patterns of pUG RNAs derived from *mCherry* (left) and *gfp* (middle) sequences in animals with single-copy transgenes (*iT*, *iTnew*, *T*, *iTswap*, and *giTswap; hrde-1(-)*) or without (wild type). The poly-UAG region of *gsa-1* mRNA serves as a positive control (right). (C) Heatmap of pUG RNA patterns detected in total RNA isolated from biological replicates of strains in (B) created by summing the intensities of amplified DNA from 0.1 to 1 kb into 7 size bins and assigning each bin a relative intensity per lane. See Supporting Information for details.

References.

1. D. L. Nanney, Epigenetic Control Systems. *Proc Natl Acad Sci U S A* **44**, 712-717 (1958).
2. A. M. Jose, Heritable epigenetic changes are constrained by the dynamics of regulatory architectures. *eLife* **12**, RP92093 (2024).
3. N. Frolov, A. Ashe, Small RNAs and chromatin in the multigenerational epigenetic landscape of *Caenorhabditis elegans*. *Philos Trans R Soc Lond B Biol Sci* **376**, 20200112 (2021).
4. S. Devanapally *et al.*, Mating can initiate stable RNA silencing that overcomes epigenetic recovery. *Nat Commun* **12**, 4239 (2021).
5. B. A. Buckley *et al.*, A nuclear Argonaute promotes multigenerational epigenetic inheritance and germline immortality. *Nature* **489**, 447-451 (2012).
6. J. Pak, A. Fire, Distinct populations of primary and secondary effectors during RNAi in *C. elegans*. *Science* **315**, 241-244 (2007).
7. A. Shukla *et al.*, poly(UG)-tailed RNAs in genome protection and epigenetic inheritance. *Nature* **582**, 283-288 (2020).
8. G. Cavalli, E. Heard, Advances in epigenetics link genetics to the environment and disease. *Nature* **571**, 489-499 (2019).
9. N. Shugarts *et al.*, SID-1 regulates a retrotransposon-encoded gene to tune heritable RNA silencing. *bioRxiv* 10.1101/2021.10.05.463267 (2023).
10. C. Frokjaer-Jensen *et al.*, Single-copy insertion of transgenes in *Caenorhabditis elegans*. *Nat Genet* **40**, 1375-1383 (2008).
11. N. O. Burton, K. B. Burkhardt, S. Kennedy, Nuclear RNAi maintains heritable gene silencing in *Caenorhabditis elegans*. *Proc Natl Acad Sci U S A* **108**, 19683-19688 (2011).
12. S. G. Gu *et al.*, Amplification of siRNA in *Caenorhabditis elegans* generates a transgenerational sequence-targeted histone H3 lysine 9 methylation footprint. *Nat Genet* **44**, 157-164 (2012).
13. R. M. Alcazar, R. Lin, A. Z. Fire, Transmission dynamics of heritable silencing induced by double-stranded RNA in *Caenorhabditis elegans*. *Genetics* **180**, 1275-1288 (2008).
14. M. Shirayama *et al.*, piRNAs initiate an epigenetic memory of nonself RNA in the *C. elegans* germline. *Cell* **150**, 65-77 (2012).
15. D. R. Knudsen-Palmer, P. Raman, F. Ettefa, L. Ravin, A. M. Jose, Target-specific requirements for RNA interference can arise through restricted RNA amplification despite the lack of specialized pathways. *bioRxiv* 10.1101/2023.02.07.527351 (2024).
16. M. A. Tuli, A. Daul, T. Schedl, *Caenorhabditis* nomenclature. *WormBook* **2018**, 1-14 (2018).
17. M. Chey, A. M. Jose, Heritable epigenetic changes at single genes: challenges and opportunities in *Caenorhabditis elegans*. *Trends Genet* **38**, 116-119 (2022).

Supplementary Information

Evidence for multiple forms of heritable RNA silencing

Mary S. Chey, Pravrutha Raman, Farida Ettefa, and Antony M. Jose*.

Department of Cell Biology and Molecular Genetics, University of Maryland, College Park, MD 20742.

*Corresponding author: Antony M. Jose

Extended Materials and Methods

Strains. Different stable phenotypes associated with the same genotype are designated as epigenetic states using a nomenclature that includes a brief description of history as proposed earlier [1].

name	shorthand (if any)	genotype {Epi-locus(e-allele [history])}
N2	+/+	wild type
GE1708		<i>dpy-2(e8) unc-4(e120)</i> II
EG4322		<i>ttTi5605</i> II; <i>unc-119(ed9)</i> III
EG6787	<i>T</i>	<i>oxSi487</i> [mex-5p::mCherry::h2b::tbb-2 3'utr::gpd-2 operon::sl2::gfp::h2b::cye-1 3'utr + unc-119(+)] II {Epi-oxSi487(e-jam1 [both mCherry::H2B and GFP::H2B were expressed upon insertion of oxSi487 using MosSCI])}
AMJ552	<i>iT</i>	<i>oxSi487 dpy-2(jam33[*e8])</i> {Epi-oxSi487(e-jam2 [both mCherry::H2B and GFP::H2B were silenced by mating males with expressed copies of oxSi487 to wild-type hermaphrodites without the transgene and then re-homozygosing the silenced transgene])}
AMJ1652	<i>iTnew</i>	<i>jamSi83</i> [mex-5p::mCherry::h2b::tbb-2 3'utr::gpd-2 operon::sl2::gfp::h2b::cye-1 3'utr + unc-119(+)] II {Epi-jamSi83(e-jam3 [both mCherry ::H2B and GFP::H2B were silenced upon insertion of jamSi83 using MosSCI])}
AMJ581	<i>T dpy-2(-)</i>	<i>oxSi487 dpy-2(e8)</i> II; <i>unc-119(ed3)?</i> III {Epi-oxSi487(e-jam1 [expression of both mCherry::H2B and GFP::H2B from oxSi487 was preserved by mating hermaphrodites with the transgene to males with dpy-2(e8) unc-4(e120)/++ males and selecting oxSi487 dpy-2(e8) animals])}
AMJ1665	<i>Tnew; hrde-1(-)</i>	<i>jamSi83; hrde-1(jam303)</i> {Epi-jamSi83(e-jam4 [both mCherry::H2B and GFP::H2B were re-expressed upon introducing a premature stop codon into hrde-1 in AMJ1652])}
AMJ844	<i>iT dpy-2(-)</i>	<i>oxSi487 dpy-2(e8)</i> {Epi-oxSi487(e-jam2)}
AMJ1208	<i>mCherry::mex-5</i>	<i>mex-5(jam197[Pmex-5::mCherry::mex-5::mex-5 3'utr])</i>
AMJ1629	<i>iTswap</i>	<i>jamSi79</i> [mex-5p::gfp::h2b::tbb-2utr::mCherry::h2b::cye-1utr] II {Epi-jamSi79(e-jam5 [both GFP::H2B and mCherry::H2B were silenced upon insertion of jamSi79 using MosSCI])}
AMJ1793	<i>giTswap; hrde-1(-)</i>	<i>jamSi79; hrde-1(jam342)</i> {Epi-jamSi79(e-jam6 [mCherry::H2B, but not GFP::H2B, was selectively re-expressed upon introducing a premature stop codon into hrde-1 in AMJ1629])}
AMJ1794	<i>giTswap; hrde-1(-); rde-3(-)</i>	<i>jamSi79; hrde-1(jam342); rde-3(jam343)</i> {Epi-jamSi79(e-jam7 [mCherry::H2B, but not GFP::H2B, was selectively re-expressed upon introducing a premature stop codon into rde-3 in AMJ1793])}
AMJ1795	<i>giTswap; hrde-1(-); znx-1(-)</i>	<i>jamSi79; hrde-1(jam342); znx-1(jam344)</i> {Epi-jamSi79(e-jam8 [mCherry::H2B, but not GFP::H2B, was selectively re-expressed upon introducing a premature stop codon into znx-1 in AMJ1793])}
AMJ1796	<i>giTswap; hrde-1(-); deps-1(-)</i>	<i>jamSi79; hrde-1(jam342); deps-1(jam345)</i> {Epi-jamSi79(e-jam9 [mCherry::H2B, but not GFP::H2B, was selectively re-expressed upon introducing a premature stop codon into deps-1 in AMJ1793])}
AMJ1421	<i>mCherry::mex-5; giT dpy-2(-)</i>	<i>oxSi487 dpy-2(e8); mex-5(jam197)</i> {Epi-oxSi487(e-jam10 [expression of mCherry::H2B, but not GFP::H2B, was selectively re-activated upon multi-generational exposure to mex-5(jam197)])}

Oligonucleotides. Primers used for RT or PCR, crRNAs and homology repair templates used for Cas9-mediated genome editing are indicated below.

name	sequence	use
P1	ataaggaggttcacgccccag	genotyping of operon variants [<i>oxSi487</i> , <i>jamSi83</i> , and <i>jamSi79</i>]
P2	ctagtgagtcgtattataagtg	
P3	tgaagacgacgagccacttg	
P4	gtgtcgaagtgtctcgacg	genotyping <i>hrde-1(jam342)</i>
P5	acggtatccaccacgagag	
P6	cgtctaacaactcccttgc	genotyping <i>rde-3(jam343)</i>
P7	ccacgttggattgtcttcg	
P8	tccgttgacagaggttacatgc	genotyping <i>deps-1(jam345)</i>
P9	agcgttccagcagaaatg	
P10	cacaacggctcgatacaagg	genotyping for <i>znfx-1(jam344)</i>
P11	cgttctgcccgttgcattcc	
P12	gctatggctgttcatggcgccatattctacttacacacacacacacaca	Reverse Transcription primer for detecting pUG signatures
P13	gctatggctgttcatggc	reverse adapter 1 for detecting pUG signatures
P14	ggcgtcgccatattctactt	reverse adapter 2 for detecting pUG signatures
P15	gagttctacgatcacattct	Primers for amplification of <i>gsa-1</i> controls when looking for pUG signatures
P16	cacttgctgaaagacaagg	
P17	atggtctccaaggggagag	Primers for detecting pUG signatures from mCherry
P18	gagaggaggataacatggct	
P19	atagatcaaaggagaagaactttca	Primers for detecting pUG signatures from gfp
P20	ttcactggagttccca	
P21	gaaaguuucaacgcguuuua	crRNA for introducing premature stop into <i>rde-3</i>
P22	cagacguuuggcuauacgcc	crRNA for introducing premature stop into <i>deps-1</i>
P23	aaugaggauuacuuacaauu	crRNA for introducing premature stop into <i>hrde-1</i>
P24	cauuauauaggcgccgucu	crRNA for introducing premature stop into <i>znfx-1</i>
P25	cgttcacaaatttaacggaaagttcaatgagtttaaggatcacgaggacattca	HRT for introducing premature stop into <i>rde-3</i>
P26	gcgaccctgtcgaggccagacgttgactatacgccctggattcgattcgaaactaccatg	HRT for introducing premature stop into <i>deps-1</i>
P27	aaagctcaacaatgaggattactataatttggtaatgccacattcccacgtttctcc	HRT for introducing premature stop into <i>hrde-1</i>
P28	gcgaccctgtcgaggccagacgttgactatacgccctggattcgattcgaaactaccatg	HRT for introducing premature stop into <i>znfx-1</i>
P29	ggcagaatgtacaagactcg	Genotyping transgenes
P30	gctgcagcccttaatgc	after integration using MosSCI
P31	gaagggcgccttaactttg	

Plasmids. For making *gfp*-dsRNA ([2] gift from the Hamza lab (University of Maryland, School of Medicine) and verified using Sanger sequencing by Ed Traver, Jose lab) or *mCherry*-dsRNA, *gfp* and *mCherry* cDNA sequences were cloned into the pL4440 vector backbone, which has flanking T7 promoters, and transformed into HT115 *E. coli*. The *mCherry*-dsRNA plasmid was created by amplifying the *mCherry* exon

sequences from EG6787 and then using Gibson Assembly (NEBuilder HiFi DNA Assembly Master Mix, New England Biolabs (NEB)). The resulting plasmid was verified using Sanger sequencing.

For homology repair after *Mos1* excision, the operon sequences were amplified from pCFJ359 (containing the sequences of *T* [3]) and pSD5 (containing the sequences of *Tcherry* [4]) using Phusion High Fidelity polymerase (NEB, catalog no. M0530S) and cloned using Gibson Assembly followed by transformation into DH5 α *E. coli*. Single colonies were isolated, and sequences were verified using Sanger sequencing.

Feeding RNAi. Animals were exposed to dsRNA targeting either *gfp* or *mCherry* only in the P0 generation as described for *gfp*-dsRNA in Devanapally et al. [4]. Briefly, worms were grown at 20°C on nematode growth media (NGM) plates supplemented with 1 mM IPTG (Omega Bio-Tek) and 25 μ g/ml Carbenicillin (MP Biochemicals). Age-matched P0 animals were fed control RNAi (HT115 bacteria with pL4440), *mCherry*-dsRNA or *gfp*-dsRNA for 24 hrs post L4, and controls were scored alongside. P0 animals and their untreated descendants growing on OP50 were analyzed for *mCherry*::H2B and GFP::H2B expression from *T*. L4-staged animals were scored in each generation by imaging (except F2 animals after *gfp* RNAi, which was scored by eye). Unimaged L4 siblings were passaged without bias in each generation to obtain progeny for the next generation.

Strain creation. Genetic crosses, *Mos1*-mediated single copy insertion (MosSCI) [5], or Cas9-mediated genome editing were used for creating various strains. In cases where a locus was susceptible to mating-induced silencing, care was taken to preserve the susceptible transgene in hermaphrodites to avoid such silencing [4].

Genetic crosses. L4-staged males (~9 animals) containing *mCherry*::*mex-5* were crossed with *iT dpy-2(-)* hermaphrodites (3 animals). F1 L4-staged nonDpy hermaphrodites and males were isolated and either imaged as L4-staged or 24-48 hours post L4 animals. Isolated F1 nonDpy hermaphrodites were also allowed to lay self-progeny. F2 hermaphrodites were singled out, allowed to lay progeny, and genotyped after ~3.5 days to identify *mCherry*::*mex-5*; *iT dpy-2(-)* homozygotes. F3 hermaphrodites were similarly passaged and genotyped to confirm homozygosity. Subsequent generations were obtained through unbiased passaging of animals and unpassaged siblings were imaged in each generation.

MosSCI. EG4322 adult animals were injected 24 hours after the L4 stage with a 10 μ l mix containing pCFJ601 (50 ng/ μ l), pMA122 (10 ng/ μ l), and a plasmid-containing operon of interest (55-60 ng/ μ l). Injected animals were isolated one to a plate and allowed to have progeny. After ~10 days, when the plate was crowded with starved animals, they were screened for nonUnc animals. The nonUnc animals were subject to heat shock in a water bath at 34°C for 2.5 hrs. After 2-3 days of recovery at 20°C, remaining nonUnc animals, if any, were isolated onto NGM plates and allowed to have progeny. Each parent nonUnc hermaphrodite was lysed and the lysates were split three ways to genotype for the left junction (P29 and P31) and right junction (P2 and P30) of integration, as well as for homozygosity (P29 and P30). Genomic DNA was prepared from plates of animals with successful MosSCI integration, and different primer sets were used to amplify the entire integrated sequence by PCR for Sanger sequencing. Sequencing of the operon inserts revealed no mutations anywhere except a mis-sense mutation within the *h2b* sequences (*his-58*: c.C314T | p.A105V) fused with *gfp* in AMJ1629. The relevance of this mutation for the observations on *Tswap*, if any, is unknown.

Cas9-mediated genome editing. Adult animals were injected 24 hours after the L4 stage with 10 μ l mix containing tracrRNA (~9 pmol/ μ l), crRNA for the gene of interest (~10-47 pmol/ μ l), *dpy-10* crRNA (~30 pmol/ μ l) or pRF4 (40 ng/ μ l), and Cas9 protein (1.6 pmol/ μ l; PNA Bio catalog no. CP01). Homology templates for generating *dpy-10(-)* were single-stranded DNA oligos [4]. However, homology templates to generate *mCherry*::*mex-5* were amplified from plasmids containing the reporter sequence using Phusion High Fidelity polymerase (New England Biolabs catalog no. M0530S) and gene-specific primers with ~35 bp of overhang homologous to the site of integration. PCR products were purified using NucleoSpin Gel and PCR Clean-up (Macherey-Nagel, catalog no. 740609.250).

Imaging. Animals of the L4 stage or between 24-72 hours after the L4 stage were mounted on a slide after paralyzing them using 3 mM levamisole (Sigma-Aldrich, Cat# 196142), imaged under non-saturating conditions (Nikon AZ100 microscope and Photometrics Cool SNAP HQ2 or Prime BSI Express camera), and categorized into a maximum of three groups (bright, dim and off). A C-HGFI Intensilight Hg Illuminator was used to excite GFP (filter cube: 450 to 490 nm excitation, 495 nm dichroic, and 500 to 550 nm emission)

or mCherry (filter cube: 530 to 560 nm excitation, 570 nm dichroic, and 590 to 650 nm emission). Sections of the gonad that were not obscured by autofluorescence from the intestine were examined to classify GFP and mCherry fluorescence. The expression of mCherry::MEX-5 after mating-induced silencing or *trans* silencing was categorized as 'on' only if fluorescence was visible when the LUTs were adjusted to a range of 0-5,000. Intestinal autofluorescence was more appreciable when imaging GFP than when imaging mCherry. In the case where fluorescence was scored by eye (F2 animals after *gfp*-dsRNA feeding), it was done at fixed magnification and zoom using an Olympus MVX10 microscope for GFP (filter cube: 460 to 480 nm excitation, 485 nm dichroic, and 495 to 540 nm emission) and mCherry (filter cube: 535 to 555 nm excitation, 565 nm dichroic, and 570 to 625 nm emission). Representative worm images were adjusted to different brightness/contrast to view different germline gene expression patterns using FIJI (NIH). All images being compared were identically adjusted for display.

pUG signatures. DNA amplicons corresponding to pUG RNA populations were amplified essentially as described in Shukla et al. [6] with the additional analysis of final patterns of the amplified populations using FIJI (NIH, version 2.4.0). All worm strains were grown on 35 mm NGM plates at 20°C seeded with 100 μ l of *E. coli* OP50. Just before all the *E. coli* was consumed, ~6 plates of worms were washed three times with M9 buffer and pooled using centrifugation at 14,000 rpm for 30 sec after each wash, yielding a ~100 μ l pellet of worms. The worm pellet was then mixed with 1 ml of TRIzol (Fisher Scientific) and subject to 3 freeze/thaw cycles in liquid nitrogen. RNA was extracted according to manufacturer's protocol using chloroform and precipitated along with 1-2 μ l of glycogen (5 μ g/ μ l in Ambion cat. #AM9510 or 20 μ g/ μ l in Invitrogen cat. #10814-010). Reverse transcription was performed using Superscript III (Invitrogen) and RT primer P12 using ~2000 ng of total RNA. Subsequent nested PCR was performed using ~2 μ l of cDNA with the first round of amplification done using Phusion Taq Polymerase (NEB) in a final reaction volume of 20 μ l for 25 cycles. The first set of gene-specific forward primers were used for each target gene (*mCherry* – P17, *gfp* – P19, and *gsa-1* – P15) with the adapter 1 reverse primer (P13). The PCR product from round 1 was diluted 100-fold and 1 μ l of the diluted product was used for the second round of PCR in a total reaction volume of 50 μ l. The second set of gene-specific forward primers (*mCherry* – P18, *gfp* – P20, and *gsa-1* – P16) were used with adapter 2 reverse primer (P14). The PCR products (~20 μ l for *mCherry* and *gfp*, and ~8 μ l for *gsa-1*) were combined with 6X loading dye, run on a 1% agarose gel and imaged using GelDoc (BioRad). All gels included an N2 control from which only a *gsa-1* amplicon is expected. A screenshot was used to generate a .png file of each gel before quantifying pUG signatures. The intensities of all bands were measured using a line of similar length through the middle of each lane using the 'Plot Profile' tool in FIJI (NIH) and processed using a custom script (R, version 4.2.2) to obtain a final heatmap (Fig. 2C). For the heatmap, the intensities of the N2 lane were subtracted from that at the corresponding positions of each sample lane (background subtraction). These background-subtracted intensities were then combined into 7 bins ranging from above the largest band of a 100-bp DNA ladder (NEB). The specific bins for all gels in arbitrary units of distance are as follows: one = 1 to 70, two = 71 to 100, three = 101 to 150, four = 151 to 180, five = 181 to 220, six = 221 to 260, and seven = 261 to 'bottom'. The 'bottom', which is just below ~100 bp, varied slightly for each pair of gels: 309 for *gfp*, 294 for *mCherry* and 296 for *gsa-1*. These binned intensities were then normalized for each lane by dividing each intensity by the maximal for that lane. With these normalized data, the heatmap was generated by setting maximum to black and minimum to white for each lane. While intensities cannot be compared across different genes because of differences in PCR efficiency, characteristic patterns for the same gene in a strain that remain comparable across biological replicates reveal the pUG signature for that gene in that strain.

Statistics. When two categories (on or off) were present in both datasets being compared, Wilson's estimates for single proportions was used and when more than two categories were present (on, off, and dim), the χ^2 test was used [4].

SI References

1. M. Chey, A. M. Jose, Heritable epigenetic changes at single genes: challenges and opportunities in *Caenorhabditis elegans*. *Trends Genet* **38**, 116-119 (2022).
2. S. Devanapally, S. Ravikumar, A. M. Jose, Double-stranded RNA made in *C. elegans* neurons can enter the germline and cause transgenerational gene silencing. *Proc Natl Acad Sci U S A* **112**, 2133-2138 (2015).
3. C. Frokjaer-Jensen, M. W. Davis, M. Ailion, E. M. Jorgensen, Improved Mos1-mediated transgenesis in *C. elegans*. *Nat Methods* **9**, 117-118 (2012).
4. S. Devanapally *et al.*, Mating can initiate stable RNA silencing that overcomes epigenetic recovery. *Nat Commun* **12**, 4239 (2021).
5. C. Frokjaer-Jensen *et al.*, Single-copy insertion of transgenes in *Caenorhabditis elegans*. *Nat Genet* **40**, 1375-1383 (2008).
6. A. Shukla *et al.*, poly(UG)-tailed RNAs in genome protection and epigenetic inheritance. *Nature* **582**, 283-288 (2020).